International Journal of Science and Research (IJSR)
ISSN: 2319-7064
SJIF (2022): 7.942

Development of Hydroxy Ethyl Cellulose based (HEC) Gold Nanocomposites Hydrogels for Antimicrobial Application

Alvakonda Narayanamma

Research Scholar, Department of Polymer Science & Technology, Sri Krishnadevraya University, Anantapur-515003
Email: *nari.prabhu[at]gmail.com*

Abstract: ***The presence of gold nanoparticles in the HEC film is confirmed by UV-Vis spectroscopy, Fourier Transform Infrared (FTIR) spectroscopy and X-ray Diffraction (XRD) analysis. The Scanning Electron Microscopic (SEM) images provide the information embedded gold nanoparticles throughout the films. In addition, the formed gold nanoparticles have an average particle size of gold and silver are estimated to be about 5 and 8 nm observed by Transmission Electron Microscopy (TEM). The anti-microbial activity of the gold nanoparticle films has demonstrated significant effects against Escherichia coli (E. coli) and Bacillus. The present study illustrates novel antimicrobial films which are potentially useful in treating infections.***

Keywords: HEC film, Gold nanoparticles, anti-microbial

1. Introduction

Nanotechnology deals with structures ranging from approximately 1 to 100nm in at least one dimension. Bulk chemicals have specific physicochemical characteristics effect is attributed to high surface area to volume ratio, which potentially results in high reactivity. Because of these, the use of these substances in nanoform may have advantages over the use of bulk chemicals.

The current trend in nanotechnology research is to use biocompatible or biological friendly polymers which can provide reduction and stabilization functions in the preparation of gold nanoparticles.

Natural polymers like starch [1, 2–8], chitosan [9], and cellulose [10–12] were reported to stabilize gold nanoparticles. Nanocomposite films possessed good mechanical properties and thermal stability, both of which are comparable to the pure cellulose films.

Films based on biopolymers function as barriers against moisture, oxygen, aroma flavor as well as oil and have future applications [13]. In addition have supports for antimicrobial, nutritional and antioxidant substances.

Bimetallic nanocomposite hydrogels form nanocomposite functional materials, comprises a metallic core covered with a shell of another metal. Durango *et al*. [14] developed edible antimicrobial films using yarn starch and chitosan and effective against S. enteritidis. Tripathi *et al.* [15] prepared chitosan- PVA blend films for food packaging applications and they have also shown to possess antimicrobial activity against food pathogenic bacteria Metal nanoparticles (either Ag or Au) do not act via cell receptors to kill the micro organisms.

Hydroxyethyl cellulose (HEC) is a derivative of cellulose with excellent water solubility and biocompatibility. It is used in many biotechnological, biophysical, and Industrial fields. In Hydroxyethyl cellulose (HEC) the ethyl group replaces one or more of three hydroxyl groups, which are present in each glucopyranoside. Hydroxyl groups on the HEC backbone reduce the silver metal ions to florets of 5 - 10 μM and acts as a capping agent. Because of the existence of abundant reactive –OH groups on the HEC chains, HEC is liable to be modified to derive new materials with improved properties.

Hydroxyethyl cellulose (HEC) reduces the Au^{3+} ions to Au^{0} nanoparticles. Hydroxyethyl cellulose (HEC), an ecofriendly polymer, is used as both reducing and stabilizing agents in the synthesis of stable gold nanoparticles. Hydroxyethyl cellulose (HEC) products are water-soluble polymers that thicken, form films, exhibit pseudoplastic solution behavior, tolerate salts and retain water.

2. Materials and Experimental Methods

Preparation of Au -metallic HEC nanocomposite films
1g/ 2g/ 3g of HEC was dissolved in 100 ml 0.25N NaOH solution and stirred for 6 h. 2ml of gold chloride ($HAuCl_4$. X H_2O) (400mg/150 ml aqueous solutions), 6 ml of MBA(1%) solution and 6 mL of APS (1%) solution were added at 25°C. This solution was kept in the sunlight for 1 h and the solution turned into brownish black color indicating the formation of nanoparticles. The solution was then poured onto Teflon covered glass plates and dried as explained earlier. Finally, the dried film was cut into the required size for further studies. The feed Composition of the gels prepared is shown in Scheme 2.

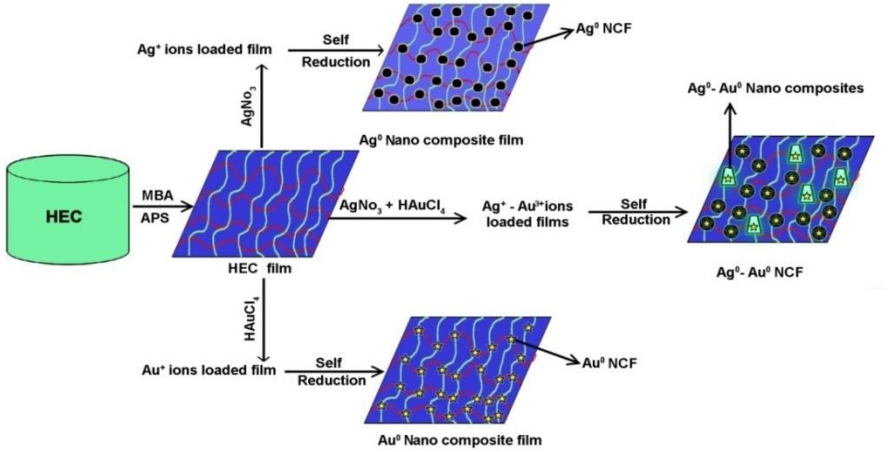

The details of materials used the methods of preparation of films and the other characterization techniques are all given in detail in Materials, Methods and characterization techniques. The Preparation of biodegradable HEC films with their code number and their feed compositions are presented in table

Table: The details code numbers of biodegradable P (AM-BPE) hydrogels and their feed compositions

Sample code	HEC(gm)	$HAuCl_4$(mL)	MBA(mL)	APS(mL)
HEC_1	1	---	6	6
HEC_2	2	---	6	6
HEC_3	3	---	6	6
$(HEC+Au^0)_1$	1	2	6	6
$(HEC+Au^0)_2$	2	2	6	6
$(HEC+Au^0)_3$	3	2	6	6

3. Result and Discussion

3.1 Swelling properties

The nanoparticle formation depends principally on the swelling behaviour of films. The results in Fig.1show that the values of the swelling characteristics were influenced by the films concentration. With an increase in the Hydroxyethyl cellulose (HEC) concentration results in increasing in the swelling ratio values of the bimetallic nanocomposite films due to the hydrophilic nature of HEC. However, bimetallic nanocomposite films have higher swelling ratios, when compared to the conventional HEC films. The reason being due to self reduction, many Au^{3+} are added that led to the formation of the nanocomposite within the films.

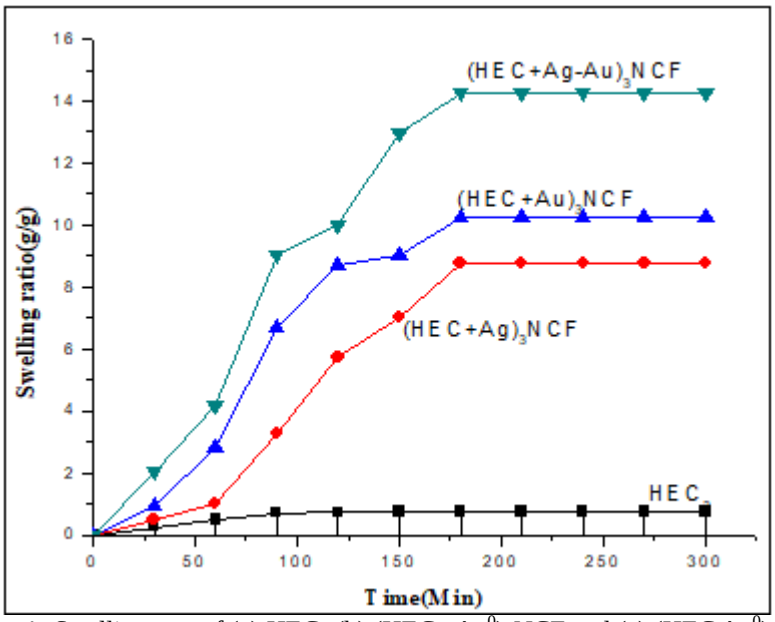

Figure 1: Swelling rate of (a) HEC_3 (b) $(HEC+Au^0)_3$NCF and (c) $(HEC\ Au^0)_3$NCF

Film code	HEC_3	$(HEC\text{-}Au^0)_3$NCF	$(HE\text{-}Au^0)_3$NCF
Swelling ratio(g/g)	0.75	10.25	14.25

3.2 Fourier transform infrared (FTIR) spectroscopy analysis

Fig. 2 shows the FTIR spectra of HEC_3, single metallic $(HEC+Au^0)_3$ and nanocomposite films. The spectrum of the HEC films shows a broad absorption band at 3491 cm^{-1} that

is related to the asymmetric and –OH symmetric stretching vibrations, the bands at 2935 -2825 cm^{-1} are attributed to stretching vibrations of the $–CH_3$ unit and the absorption band at 1656 cm^{-1} is from the carbonyl groups of the HEC films. The other main characteristic peaks of HEC at 1113-1118 cm^{-1} were assigned to the carbonyl group. However, these peaks shifted in the case of the single metallic $(HEC+Au^0)_3$. Table 2 illustrates the important peaks observed for the single metallic $(HEC+Au^0)_3$. Overall, the shifting of the peaks confirms the formation of nanoparticles with HEC_3.

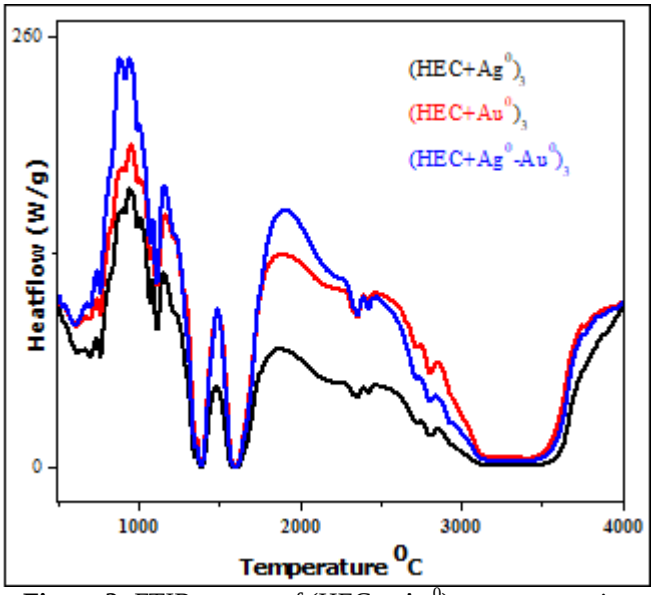

Figure 2: FTIR spectra of $(HEC + Au^0)_3$ nanocomposite films

Table 2: Fourier transform infrared spectral data of the HEC based films

Film Code	FTIR bands (cm^{-1})
$(HEC\text{-}Au^0)_3$	3479, 2825, 2704, 2353, 1590, 1408, 1118, 706

3.3 UV–Visible spectroscopy analysis of Au0 nanocomposite

The formation of Au^0 nanoparticles in the films were analyzed by comparing the UV-spectra of metallic and bimetallic nanocomposite solutions (Fig.3), formation of gold nanoparticles show a characteristic peak at 417.55 nm. Similarly, UV abortion peaks of Au^0 nanoparticles were obtained at 449.65nm which indicates the formation of as well as gold nanoparticles in the HEC film. The spectral study once again suggests that simultaneous reduction of $HAuCl_4$ in solution and giving a film containing homogeneous alloy nanoparticles.

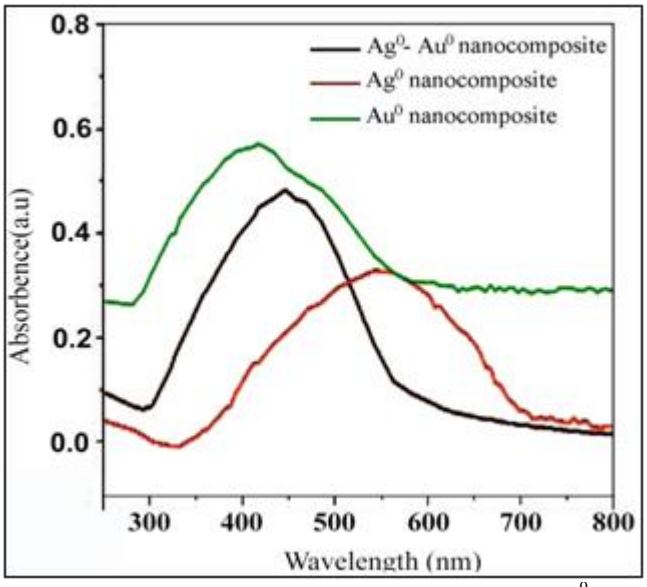

Figure 3: UV- Spectrum of nanocomposites (Au^0 nanocomposites)

3.4 Thermogravimetric Analysis (TGA)

Thermogravimetric analysis was used to study the formation of nanoparticles and the thermal stability of the different films. As shown in Fig.4 the thermal decomposition of HEC_3 and single metallic $(HEC+Au^0)_3$ nanocomposite films occurred at 625 °C with a significant mass loss of 98.12% respectively. For the nanocomposite films $(HEC + Au^0)_3$, which was due to the partial decomposition of the Au^0 nanoparticles. Moreover, according to the TGA results, the bimetallic nanocomposite films $(HEC +Au^0)_3$ showed a higher thermal stability when compared with the other films.

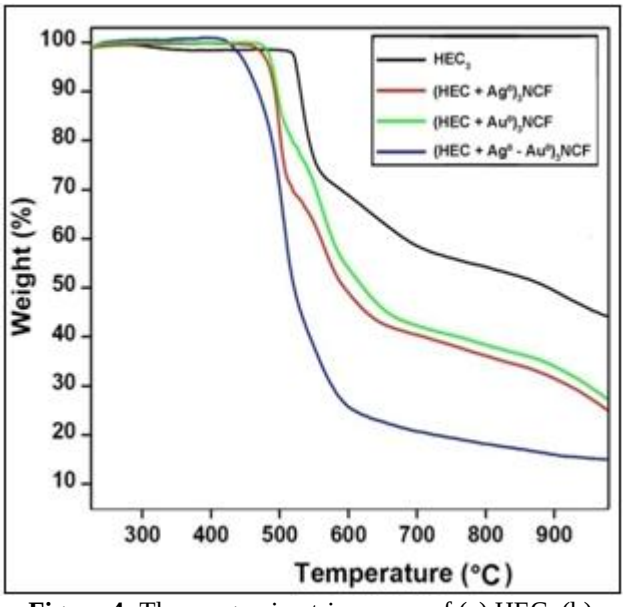

Figure 4: Thermogravimetric curves of (a) HEC_3 (b) $(HEC+Au^0)_3NCF$

3.5 X-ray diffraction studies

The X-ray diffraction study gives spotting information of nanoparticles formed in the HEC_3 film networks which shows crystalline peaks in Figure 5. However in the case of

Au nanocomposite films can exhibit 2θ highly sharp peaks at 44.52 and 64.83 when compared to other films, which can be corroborated to (111), (200), (220) and (222) reflections, due to the formation of Au^0 nanocomposite films Figure. 6(b).

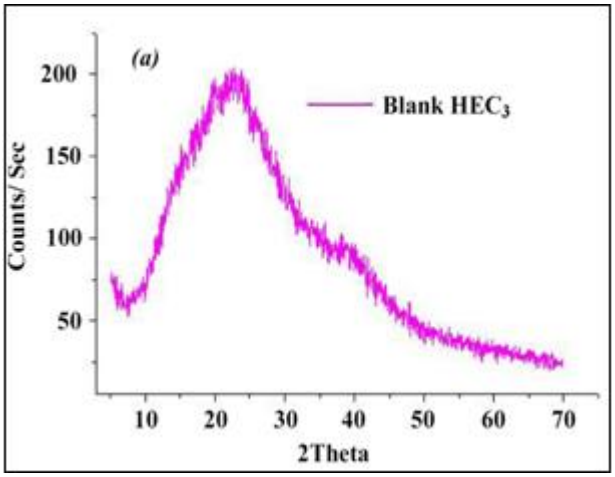

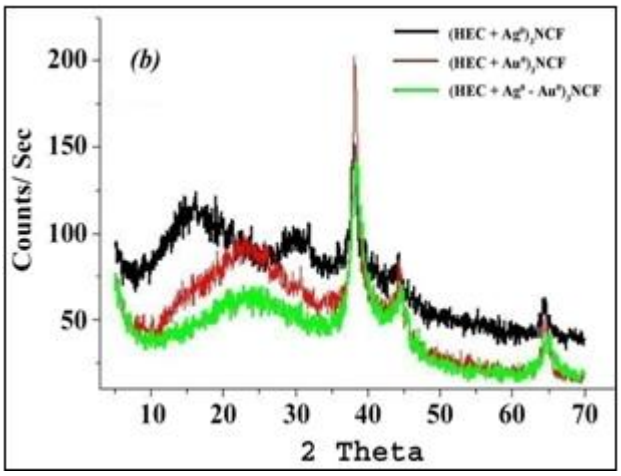

Figure 5: X-ray diffraction patterns of (a) blank HEC_3 $(HEC+Au^0)_3NCF$

3.6 Scanning electron microscopy

The structure and elemental composition of the nanoparticles were investigated by SEM. The film morphology stabilization of dependents on the HEC_3 content (Fig.6). Fig.6(a) shows formation of Au^0 nanoparticles $(HEC+Au^0)_3$ in NCF**,** it is obvious from Fig.6 (d) that a huge quantity of metallic nanoparticles was dispersed on the $(HEC+Au^0)_3$ in NCF .The same results were confirmed with optical micrograph images of SEM in Fig.6.

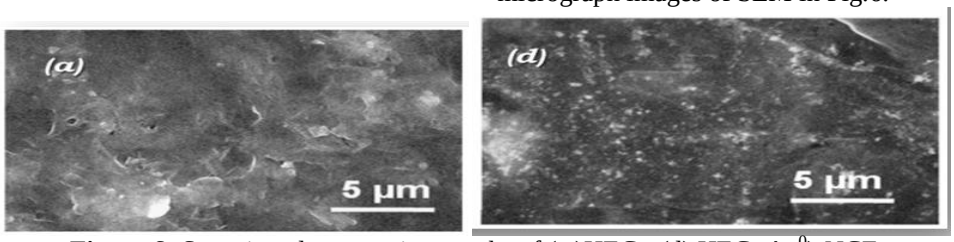

Figure 6: Scanning electron micrographs of (a)HEC_3 (d) $HEC+Au^0)_3NCF$

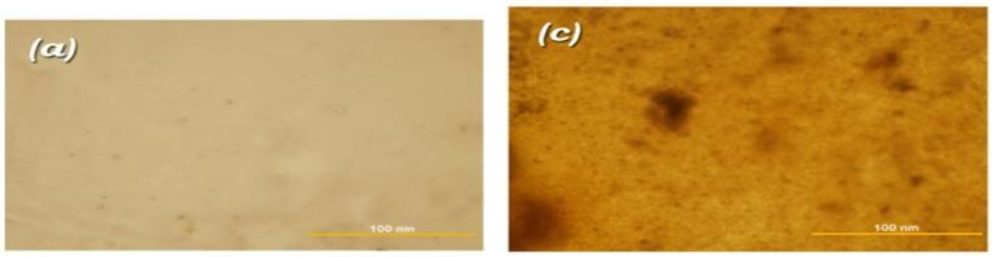

Figure 7: Optical micrograph images of (a) HEC_3, (c) $(HEC+Au^0)_3NCF$

3.7 Transmission electron microscopy (TEM) analysis

TEM images of Au^0 and bimetallic Au^0 nanoparticles on HEC_3films have an average diameter of ~20nm and their corresponding size distribution of histograms are shown in Fig.9 a respectively. The images show that all three colloidal nanoparticles have 'near monodisperse' size distributions.

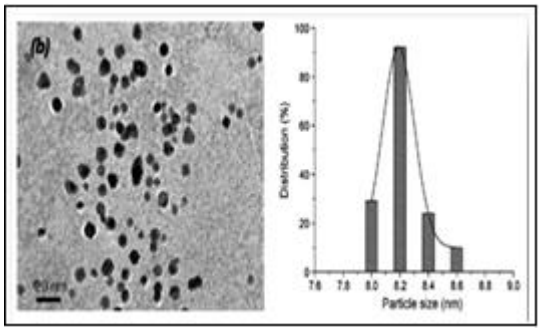

Figure 9: Transmission electron images of (a)$(HEC+Au^0)_3NCF$

3.8 Mechanical Properties

Many synthetic and natural polymeric materials are developed to treat the burn wounds and as antibacterial materials. However, they have limited applicability due to poor mechanical properties as well as lower rates of water absorption. A number of hydroxyethyl cellulose gold metallic nanocomposites have been developed for many applications. To have better mechanical strength impregnated hydroxyethyl cellulose gold metallic nanocomposites are developed in the present investigation for higher applicability. The mechanical properties of HEC_3 and $(HEC+ Au^0)_3$NCF films are presented in Table 3. The higher stress at maximum load, modulus, and elongation at break are noticed for $(HEC+ Au^0)_3$ nanocomposite film compared to HEC_3 film.

Table 3: Mechanical properties of HEC and HECNCFs

Sample code	Maximum stress (MPa)	Young's modulus (MPa)	Elongation at break (%)
HEC_3	12.52	710	1.481
$(HEC+Au^0)_3$	15.21	925	1.658

3.9 Antibacterial property test

Inorganic nanoparticles inherently possess bacteria-killing properties, but by modifying the inorganic nanoparticles these properties can be improved. Recently in the biomedical field, a synthesis of much smaller nanoparticles by a green process was developed to enhance the inactivation of bacteria by 'Inhibiting the formation of pits' mechanism. These pits cause polymer molecules and membrane proteins of the bacteria to leak, leading to microbial death. The dual nanoparticles enter into the bacteria cell more effectively, causing damage to the nuclei and resulting in faster bacterial death. The antimicrobial efficacy of the gold metallic hydrogels developed from nanoparticles was examined against Bacillus and E. coli model bacteria. The effects of the HEC_3, $(HEC + Au^0)_3$ films on bacteria are shown in Fig. 10.

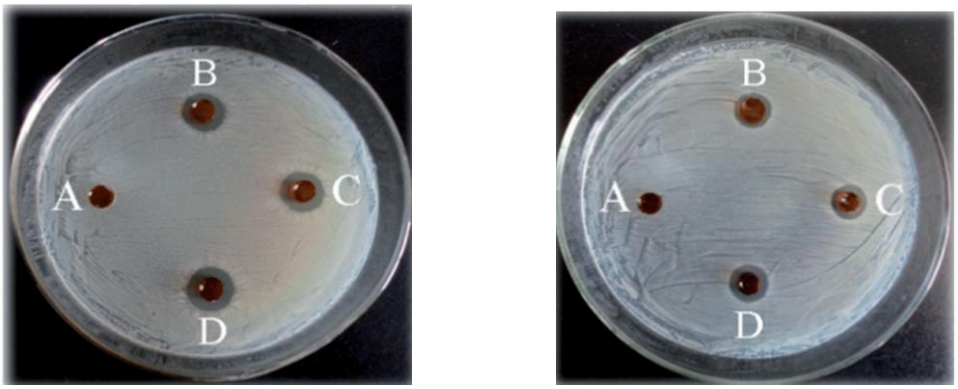

Bacillus *E.coli*

Figure 10: Antibacterial activity of (A) HEC_3 (C) $(HEC+Au)_3$ NCF against Bacillus, E. coli by disc diffusion method

4. Conclusions

In summary, it is clearly illustrated that the Au^0 nanoparticles are being formed not only on the surface of film but also throughout the networks of hydroxyethyl cellulose. The nanocomposites are analyzed by using spectral, thermal, and electron microscopy methods. They are confirmed as excellent antibacterial materials against Bacillus and Escherichia coli.

The development of synthetic and fabrication technologies for fundamental understanding of nanocomposite films will continue with a greater emphasis on designing sophisticated multi component and complex materials that can be tailored to very specific applications. Emerging new techniques strongly support the systematic characterization of nanocomposite gels which, in return, drives research forward and impacts the rational design of materials.

References

[1] Vigneshwaran,N., Nachane, R. P. , Balasubramanya, R. H. and Varadarajan, P.V., *Carbohydrate Research*, vol. 341, no. 12, (2006), pp. 2012–2018.
[2] Kassaee, M.Z., Akhavan, A., Sheikh, N., and Beteshobabrud, R., Radiation Physics and Chemistry, vol. 77, no. 9, (2008), pp. 1074–1078.
[3] Sharma, V. K., Yngard, R. A. , and Lin, Y., *Advances in* Colloid and Interface Science, vol. 145, no. 1-2,(2009), pp. 83–96.
[4] Valodkar, M., Bhadoria, A., Pohnerkar, J., Mohan, M., and Thakore, S., Carbohydrate Research, vol. 345, no. 12, (2010), pp. 1767–1773.
[5] Hebeish, A., El-Naggar, M.E., G. Fouda, M.M., Ramadan, M.A., Al-Deyab, S.S., and El-Rafie, M.H. *Carbohydrate Polymers*, Vol. 86, No. 2, (2011), pp. 936–940.
[6] El-Rafie, M.H., El-Naggar, M.E., Ramadan, M.A., G. Fouda, M.M., Al-Deyab, S.S., and Hebeish, A., *Carbohydrate Polymers*, vol. 86, no. 2, (2011), pp. 630–635.

[7] Djokovi´c, V., Krsmanovi´c, R., Bo˘zani´c, D. K. et al., Colloids and Surfaces B, Vol. 73, No. 1, (2009), pp. 30–35.
[8] Raveendran, P., Fu, J., and Wallen, S.L., *Green Chemistry*, vol. 8, no.1, (2006) pp.34–38.
[9] Huang, H., Yuan, Q., and Yang, X., "Preparation and characterization of metal-chitosan nanocomposites," *Colloids and Surfaces B*, vol. 39, no. 1-2,(2004), pp. 31–37.
[10] Chen, J., Wang, J., Zhang, X., and Jin, Y *Materials Chemistry and Physics*,vol.108, no. 2-3, (2008), pp. 421–424.
[11] Liu, W., Zhang, Z., Liu, H., He, W., Ge, X., and Wang, M., *Materials Letters*, vol. 61, no. 8-9,(2007), pp. 1801–1804.
[12] Hebeish, A.A., El-Rafie, M.H., Abdel-Mohdy, F.A., Abdel-Halim, E.S. and Emam, H.E., Carbohydrate Polymers, vol. 82, no. 3,(2010), pp. 933–941.
[13] Lu, S., Gao, W., Gu, H.Y., *Burns*, Vol. 34, No. 5, (2005), pp.623-628.
[14] Durango, A.M., Soares, N.F.F., Benevides, S., Teixeira, J., Carvalho, M., Wobeto, C., Andrade, N.J., *Packaging Technology Science*,Vol.19, No.1, (2006), pp.55-59.
[15] Tripathia, S., Mehrotra, G.K., and Dutta, P.K., International Journal of Biological Macromolecules, Vol. 45, No. 4, (2009), pp. 372-376.